styles between these two extremes may provide explanations for such diverse rifting phenomena as crustal doming, the occurrence of so called 'wet' rifts (with volcanism), and 'dry' rifts (without volcanism)[23], uplifted graben shoulders[21], apparent depth-dependent extension[28], and the apparent simple shear[29] or delamination of the lithosphere[30]. This alternative working model of continental rifting is consistent with current ideas about both the rheology of the lithsophere and the driving forces of plate tectonics.

We thank Roger Buck for constructive reviews of the manuscript.

Received 1 February; accepted 11 April 1988.

1. Milanovsky, E. E. *Tectonophysics* **15**, 65-70 (1972).
2. Sengör, A. M. & Burke, K. *Geophys. Res. Lett.* **5**, 419-421 (1978).
3. Wilson, J. T. *Nature* **207**, 343-347 (1965).
4. McConnell, R. B. *Bull. geol. Soc. Am.* **83**, 2549-2572 (1972).
5. King, B. C. in *Tectonics and Geophysics of Continental Rifts* (eds Ramberg, I. B. & Neumann, E. R.) 347-350 (Reidel, Dordrecht, 1978).
6. Fuchs, K. in *Approaches to Taphrogenesis* (eds Illies, J. H. & Fuchs, K.) 420-432 (Schweizerbart, Stuttgart, 1974).
7. Illies, J. H. in *Tectonics and Geophysics of Continental Rifts* (eds Ramberg, I. B. & Neumann, E. R.) 63-71 (Reidel, Dordrecht, 1978).
8. Sykes, L. R. *Rev. Geophys. Space Phys.* **16**, 621-688 (1978).
9. Brace, W. F. & Kohlstedt, D. L. *J. geophys. Res.* **85**, 6248-6252 (1980).
10. Meissner, R. *The Continental Crust*, 162-167 (Academic, New York, 1986).
11. Pollack, H. N. *Earth planet. Sci.* Lett. **80**, 175-182 (1986).
12. Ballard, S. & Pollack, H. N. *Earth planet. Sci. Lett.* **85** 253-264 (1987).
13. Vink, G. E., Morgan, W. J. & Zhao, W. *J. geophys. Res.* **89**, 10072-10076 (1984).
14. Dewey, J. F. in *The Nature of the Lower Continental Crust* (eds Dawson, J. B., Carswell, D. A., Hall, J. & Wedepohl, K. H.) 71-78 (Geological Society, London, 1986).
15. Chapple, W. M. *Bull. geol. Soc. Am.* **89**, 1189-1198 (1978).
16. Kirby, S. H. *Rev. Geophys. Space Phys.* **21**, 1458-1487 (1983).
17. Zienkiewicz, O. C. & Godbole, P. N. in *Finite Elements in Fluids* Vol. 1, Ch. 2 (eds Gallagher, R. H., Oden, J. T., Taylor, C. & Zienkiewicz, O. C.) (Wiley, New York, 1975).
18. Zienkiewicz, O. C. *The Finite Element Method* 93-118 (McGraw-Hill, London, 1977).
19. Walcott, A. B. *J. geophys. Res.* **75**, 3941-3954 (1970).
20. Huebner, K. H. & Thornton, E. A. *The Finite Element Method for Engineers* 423-427 (Wiley, New York, 1982).
21. Buck, W. R. *Earth planet. Sci. Lett.* **77**, 362-372 (1986).
22. Ringwood, A. E. *Composition and Petrology of the Earth's Mantle* 150-169 (McGraw-Hill, New York, 1975).
23. Barberi, F., Santacroe, R. & Varet, J. in *Continental and Oceanic Rifts, Geodyn. Ser.* Vol. 8 (ed. Palmason, G.) 293-309 (AGU, Washington, D.C., 1982).
24. Mohr, P. *Trans. Am. geophys. Un.* **68**, 721-730 (1987).
25. Jones, C. H. *Tectonics* **6**, 449-473 (1987).
26. Kerr, R. A. *Science* **239**, 978-979 (1988).
27. Burchfiel, B. C., Hodges, K. V. & Royden, L. H. *J. geophys. Res.* **92**, 10422-10426 (1987).
28. Rowley, D. B. & Sahagian, D. *Geology* **14**, 32-35 (1986).
29. Wernicke, B. *Can. J. Earth Sci.* **22**, 108-125 (1984).
30. Lister, G. S., Etheridge, M. A. & Symonds, P. A. *Geology* **14**, 246-250 (1986).

Network model of shape-from-shading: neural function arises from both receptive and projective fields

Sidney R. Lehky & Terrence J. Sejnowski

Department of Biophysics, Johns Hopkins University, Baltimore, Maryland 21218, USA

It is not known how the visual system is organized to extract information about shape from the continuous gradations of light and dark found on shaded surfaces of three-dimensional objects[1,2]. To investigate this question[3,4], we used a learning algorithm to construct a neural network model which determines surface curvatures from images of simple geometrical surfaces. The receptive fields developed by units in the network were surprisingly similar to the actual receptive fields of neurons observed in the visual cortex[5,6] which are commonly believed to be 'edge' or 'bar' detectors, but have never previously been associated with shading. Thus, our study illustrates the difficulty of trying to deduce neuronal function solely from determination of their receptive fields. It is also important to consider the connections a neuron makes with other neurons in subsequent stages of processing, which we call its 'projective field'.

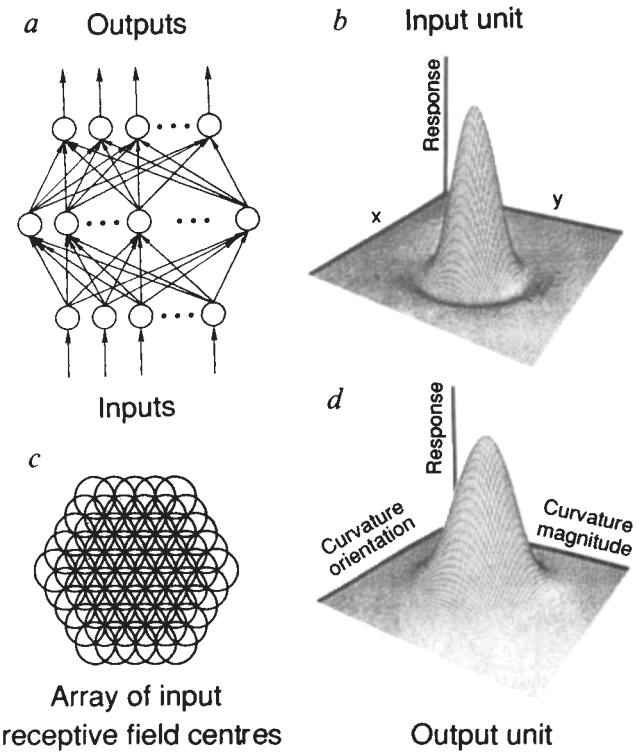

Fig. 1 Organization of neural network that extracts surface curvatures from images of shaded surfaces. *a*, Diagram of three-layer network. Each unit projects to all units in the subsequent layer. The responses of the units in the input layer are determined by the environment. The responses of each unit in the hidden and output layers are determined by summing the activities from all units in preceding layer, weighted by connection strengths which can be positive or negative, and then passed through a sigmoid nonlinearity. Unit activities can assume any value between 0.0-1.0. *b*, Input-unit receptive field, formed by the Laplacian of a two-dimensional guassian. On-centre units have an excitatory centre and an inhibitory surround, while off-centre units have opposite centre/surround polarities. The on- and off-centre terminology does not imply any temporal properties for these units. *c*, Receptive field centres of input units overlapped in a hexagonal array. Images were sampled by both on-centre and off-centre arrays, which were spatially superimposed. *d*, Output-unit response curve, tuned to both curvature magnitude and orientation. The maximum response of each output unit was produced by a different combination of those two curvature parameters. The magnitude axis is on logarithmic scale. Multi-dimensional responses such as this are common in the visual cortex for various parameters, although units selective for surface curvature have not been reported.

The specific task we set for the network was to determine the magnitudes and orientations of the two principal surface curvatures at the centre of each input surface, and to do this independently both of lateral translations of the surface within a small patch of the visual field, and also independently of the direction of illumination. Surface curvature depends upon the direction of travel along a surface. The principle curvatures are the maximum and minimum curvatures for all trajectories through a particular point, which are always perpendicular to each other, and are good descriptors of local shape.

The network had three layers (Fig. 1*a*): an input layer (122 units), an output layer (24 units), and an intermediate hidden layer (27 units). The input layer consist of arrays of units with circular receptive fields (Fig. 1*b*, *c*), similar to neurons found in the retina and the lateral geniculate nucleus. Output units were selective for both the magnitude and orientation of curvature (Fig. 2*d*). Because of its non-monotonic, tuned response, the activity of a single output unit represented the curvature

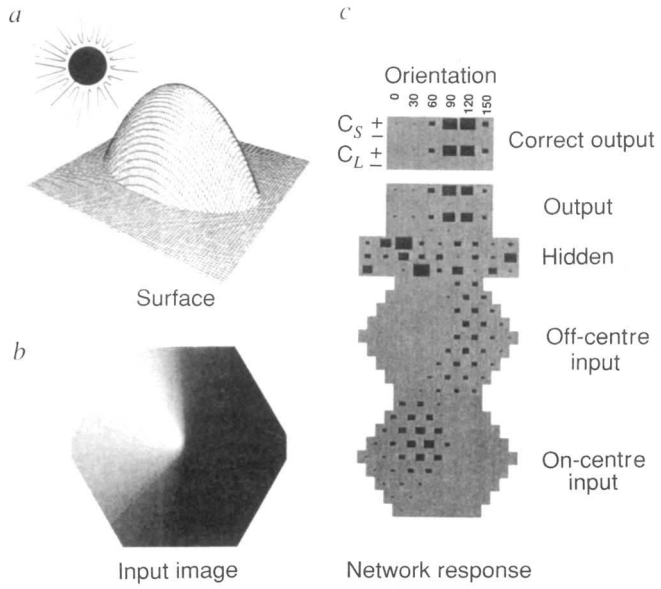

Fig. 2 Typical input image and resulting activity levels within a trained network. *a*, Example of an ellipitcal paraboloid surface. (The flat base did not fall within the input field of the network). *b*, One of 2,000 images used to train the network, synthesized by calulating light reflected from the paraboloid surface. Each image differed in the magnitudes and orientation of the two principal curvatures, in the slant and tilt of illumination, and in the location of the surface centre within the input field. All image parameters were randomly selected from a uniform distribution. The curvature magnitude ranged drom 2 deg^{-1} to 32 deg^{-1} and also -2 deg^{-1} to -32 deg^{-1}, and the curvature orientation from 0° to 180°. The centre of the paraboloid could fall anywhere within the central third of the input field, and the surface normal at the paraboloid centre was always perpendicular to the image plane. Surface reflection was Lambertian, or matte. Illumination came predominantly from one direction but was partially diffused to eliminate sharp shadow edges. The illumination slant fell between 0°–60°. The network was trained to interpret images assuming that illumination came from above (tilt between 0°–180°), and that the signs of both curvatures were the same (that is, the surface was convex or concave). *c*, The network response to an image. The area of a black square indicates a unit's activity. Double hexagons show the responses of 61 on-centre and 61 off-centre input units, calculated by convolving their receptive fields with the image. The responses were rectified, and so they only assumed positive values. These input units cause activity in the 27 hidden units, arranged in a 3×9 array above the hexagons. The hidden units in turn project to the output layer of 24 units, shown in a 4×6 array. This output should be compared with the other 4×6 array at the very top, which shows a correct response to the image. Units within a 4×6 array are arranged as follows. The six columns correspond to different peaks in orientation tuning, at 0°, 30°, 60°, 90°, 120° and 150°. The rows correspond to different curvature magnitudes: the top two rows code for positive (tuning peak: +8 deg^{-1}) and negative (tuning peak: −8 deg^{-1}) magnitudes of the smaller of the two principal curvatures (C_S), while the bottom two rows code the same for the larger principal curvature (C_L) (same tuning peaks). Curvature orientation is unambiguously coded by the pattern of activity in six overlapping orientation-tuning curves. Representation of curvature magnitude, however, remains degenerate because output unit tuning curves in that domain do not overlap. An output can therefore correspond to two curvature magnitudes, which the network cannot distinguish. This remaining ambiguity could be resolved with a larger network containing units that are responsive at different spatial scales.

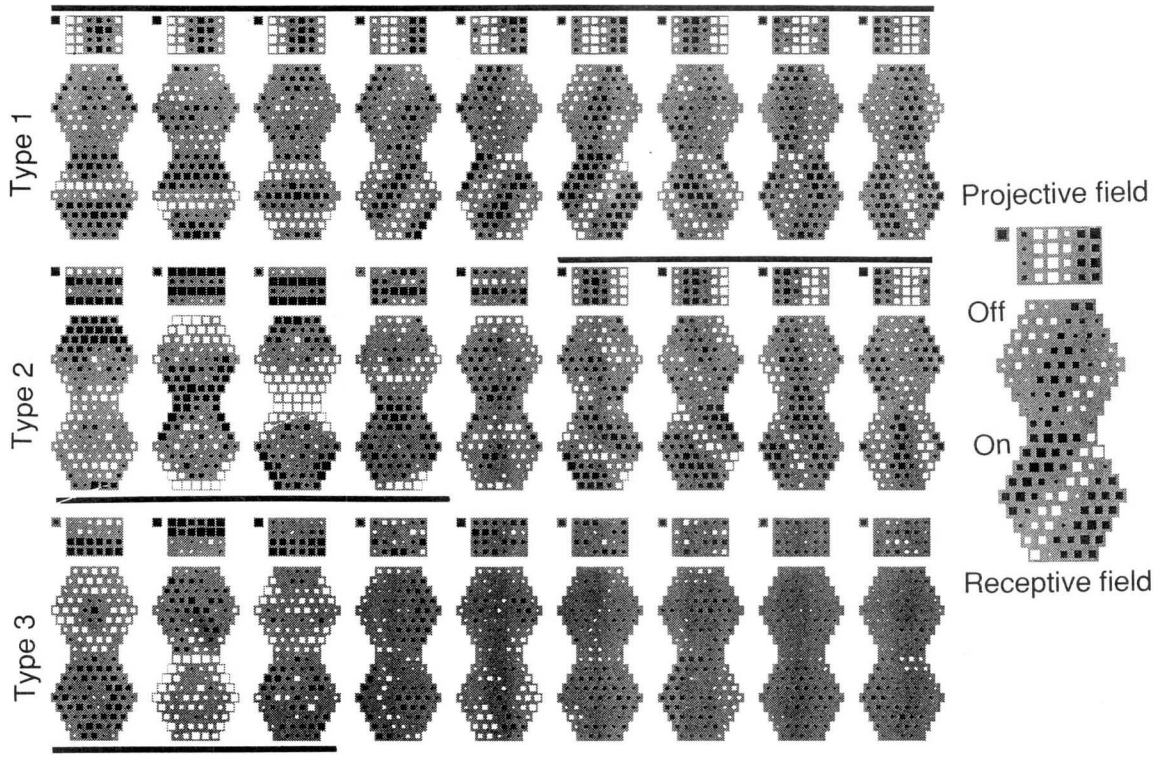

Fig. 3 Connection strength in a typical network. Excitatory weights are white and inhibitory ones are black, and the areas of the squares indicate the connection strengths. Each hidden unit is represented by one hourglass-shaped icon, showing its receptive field (double hexagons) and projective field (4×6 array at the top). The organization of units in the 4×6 array is as described in Fig. 2*c*. The isolated square at the left of each icon indicates the unit's bias (equivalent to a negative threshold). Black horizontal lines group units that have the same type of projective field organization

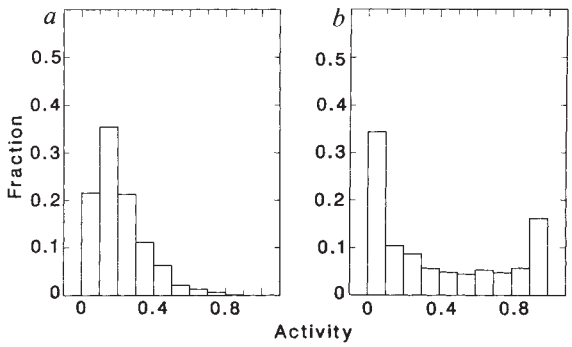

Fig. 4 Distribution of activity levels for two hidden units when the network was presented with the 2,000 images described in Fig. 2*b*. For each image, units gave responses between 0.0 and 1.0, which were grouped into ten bins. *a*, Histogram with a unimodal distribution typical of orientation-selective units (type 1) and of units selective for the relative magnitudes of the principal curvatures (type 3). These units tend to be activated over a range of intermediate levels when presented with many inputs, and appear to act as continuous, tuned filters indicating the values of their respective parameters. *b*, Histogram with typical bimodal distribution for a unit discriminating between positive and negative curvatures (type 2). These units are like feature detectors, tending to be either fully on or off to indicate whether a surface is convex or concave.

parameters in a degenerate manner; that is, various input images could lead to the same response. To resolve this ambiguity, curvature parameters were encoded by the pattern of activity in a population of output units having different, but overlapping tuning curves, analogous to the way that colour can be encoded by the pattern of activity in three broadly tuned channels. This network was intended to model processing for only a small patch of the visual field, about the size handled by a single cortical column. It would have to be replicated at different locations to cover the entire field, perhaps with all components feeding into a higher level network to integrate the local analyses.

Given this three-layer network architecture, the 'back-propagation' learning algorithm[7] was used to organize the properties of the hidden units to provide a transform between the retinotopic space of the input units and the two-dimensional magnitude and orientation parameter space of the outputs. Images of elliptic paraboloid surfaces were used as inputs (Fig. 2*a*, *b*). Sharp edges were excluded from the images, and so the only cues available for computing curvatures were in the shading. The network was presented with many images, and, for each input, responses were propagated up to the output units. The actual output was then compared with the correct output for that image, and all connection strengths in the network were slightly modified to reduce error in the manner specified by the algorithm. Gradually, the initially random connection strengths became organized. The correlation between the correct and the actual outputs reached a plateau of 0.88 after 40,000 presentations, and the network generalized well for images that were not part of the training set. Increasing the number of hidden units failed to improve the network performance, although it did deteriorate when there were too few hidden units. No biological significance is claimed for the algorithm by which the network developed but, rather, the focus of interest is on the resulting mature network.

An example of the network's response to an image is given in Fig. 2*c* and the network connection strengths underlying this response are shown in Fig. 3. Each of the 27 hourglass-shaped icons represents the connections associated with one hidden unit. The double hexagons in each icon show the connections from all input units to that hidden unit (that is, the receptive field), and the 4×6 array at the top shows the connections between that hidden unit and all output units (that is, the projective field). Repeating the learning procedure starting from completely different sets of random weights resulted in essentially the same pattern of connections.

The receptive fields in Fig. 3 are reminiscent of those in the visual cortex[5,6,8]. Excitatory and inhibitory connections are often organized in an orientation-specific and muti-lobed manner, although some are more or less circularly-symmetrical. Upon examining projective fields, however, three types become apparent: type 1 has a vertical pattern of organization to the 4×6 array of weights; type 2 has a horizontal organization with alternate rows being similar; and type 3 has a horizontal organization with adjacent rows being similar. These classes of hidden units appear to provide information to output units about, respectively, the orientation of the principal curvatures (type 1), their signs (convexity/concavity) (type 2), and their relative magnitudes (type 3). The units had different response distributions when presented with many stimuli. Type 1 and type 3 had unimodal distributions (Fig. 4*a*), whereas type 2 units had bimodal distributions (Fig. 4*b*). Based on these distributions, we interpret types 1 and 3 as being filters that indicate values for their respective parameters, and type 2 units as being feature detectors that discrminate between discrete alternatives (convexity and concavity). A few hidden units were difficult to classify, and four failed to develop large weights.

We tried probing the units with simulated bars of light and found that the responses of the hidden units were easily predictable from the pattern of excitatory and inhibitory connections they received from the input units, and that most of these responses appear similar to those of simple cells in the visual cortex[5,8]. In contrast, it required extensive trial and error to find the optimal stimulus for the output units, but this was not surprising as each output unit received convergent inputs from all 27 hidden-unit receptive fields. Some output units had strong 'end-stopped inhibition', similar to that of some complex cells in the cortex[6]. In these units, responses dropped precipitously when the bar length was extended beyond a certain point.

Examination of the receptive fields of individual units does not make apparent what the network is doing, and interpretations other than that of extracting curvatures from shaded images are likely to spring to mind. While this model network obviously does not establish that receptive fields in the cortex which resemble those developed by the network are engaged in shading analysis, it does raise questions about conventional interpretations of the functions of receptive fields, not only in visual pathways, but in other sensory systems as well. Understanding the function of a neuron within a network appears to require not only knowledge of the pattern of input connections forming its receptive field, but also knowledge of the pattern of output connections, which forms its projective field. Indeed, the same neuron may have a number of different functions if it projects to several regions.

This work was supported by an NSF Presidential Young Investigator Award to TJS and a Sloan Foundation grant to TJS and Dr G. F. Poggio.

Received 7 March; accepted 25 April 1988.

1. Ramachandran, V. S. *Nature* **331**, 163–166 (1988).
2. Mingolla, E. & Todd, J. T. *Biol. Cyber.* **53**, 137–151 (1986).
3. Ikeuchi, K. & Horn, B. K. P. *Art. Intell.* **17**, 141–184 (1981).
4. Pentland, A. P. *IEEE Transactions on Pattern Analysis and Machine Intelligence* **6**, 170–187 (1984).
5. Hubel, D. H. & Wiesel, T. N. *J. Physiol., Lond.* **160**, 106–154 (1962).
6. Hubel, D. H. & Wiesel, T. N. *J. Neurophysiol.* **28**, 229–289 (1965).
7. Rumelhart, D. E., Hinton, G. E. & Williams, R. J. in *Parallel Distributed Processing: Explorations in the Microstructure of Cognition. Vol.* 1 (eds Rumelhart, D. E. & McClelland, J. L.) 318–362 (MIT Press, Cambridge, 1986).
8. Mullikan, W. H., Jones, J. P. & Palmer, L. A. *J. Neurophysiol.* **52**, 372–387 (1984).